Anal. Chem. **1999,** *71,* 291−301

ESI/Ion Trap/Ion Mobility/Time-of-Flight Mass Spectrometry for Rapid and Sensitive Analysis of Biomolecular Mixtures

Sheila C. Henderson, Stephen J. Valentine, Anne E. Counterman, and David E. Clemmer*

Department of Chemistry, Indiana University, Bloomington, Indiana 47405

An ion trap/ion mobility/time-of-flight mass spectrometry technique is shown to be a rapid and sensitive means of analyzing peptide/protein mixtures. In this approach, an ion trap is used to accumulate ions that have been electrosprayed from a mixture into concentrated packets. The ion packets are injected into a drift tube where components of the mixture are separated based on differences in mobility through a buffer gas. Ions that exit the drift tube are dispersed in a time-of-flight mass spectrometer for mass-to-charge (m/z) determination. The gas-phase separation strategy reduces congestion in the mass spectrum, and experimental mobilities complement m/z measurements in assigning peaks. Examples of the application of the approach to identification of peptides (from tryptic digests) and to separation of charge-state distributions from electrospray of a mixture containing ubiquitin and myoglobin are presented. Most peptides that are observed from tryptic digests of proteins such as cytochrome *c* and myoglobin can be identified from data that are acquired in under 1 min; studies of mixtures with known compositions indicate that detection limits are ∼0.5−3 pmol for individual components. Factors that may influence the distributions that are observed, such as storage time in the trap, injection voltages used for the mobility experiment, and variations in ion cross section with charge state, are discussed.

Since the development of ion sources that are capable of producing intact macromolecular ions,[1,2] mass spectrometry (MS)-based methods for determining molecular weights[3,4] and sequencing[5−9] have become routinely applied to biochemical problems. A problem that arises for electrospray ionization (ESI)[1] is that mass spectra for mixtures or samples containing impurities can be difficult (or impossible) to interpret because of the multiple charging phenomenon. ESI charge-state distributions for individual components of mixtures often occur over the same narrow mass-to-charge (m/z) range such that charge states of components with different molecular weights may exhibit overlapping peaks. Many of the problems that arise from direct ESI of mixtures are eliminated by use of separation methods.[10] Here, we discuss a new separation strategy for biomolecules that is based on differences in ion mobilities in the gas phase. We show that gas-phase separations provide a rapid and sensitive means of analyzing complex mixtures of biomolecules and that complementary mobility information from the separation step is useful in assigning components of the mixture.

Numerous efforts have been made to facilitate ESI-MS analysis of electrosprayed mixtures. Algorithms for obtaining mass information directly from mass spectra for electrosprayed mixtures have been devised;[11] these work best when peaks in the mass spectrum are highly resolved and chemical noise is low. High-resolution Fourier transform ion cyclotron resonance and time-of-flight MS methods are also an effective means of analyzing mixtures. Charge states can be deduced by determining the isotopic spacing;[12] different components can be distinguished even when spacings between m/z ratios are at the parts per million level.[13] Stephenson and McLuckey stored mixtures of electrosprayed ions in traps and used ion−neutral reactions[14] to distinguish ions with similar m/z ratios and cation−anion reactions to reduce charge states[15] in order to take advantage of the larger m/z spacing between lower charge states.

(1) Fenn, J. B.; Mann, M.; Meng, C. K.; Wong, S. F.; Whitehouse, C. M. *Science* **1989**, *246*, 64.
(2) Karas, M.; Bachmann, D.; Bahr, U.; Hillenkamp, F. *Int. J. Mass Spectrom. Ion Processes* **1987**, *78*, 53. Hillenkamp, F.; Karas, M.; Beavis, R. C.; Chait, B. T. *Anal. Chem.* **1991**, *63*, 1193A.
(3) Chait, B. T.; Kent, S. B. H. *Science* **1992**, *257*, 1885.
(4) Biemann, K. *Annu. Rev. Biochem.* **1992**, *61*, 997.
(5) Biemann, K.; Scobel, H. A. *Science* **1987**, *237*, 992.
(6) Burlingame, A. L.; Boyd, R. K.; Gaskell, S. J. *Anal. Chem.* **1994**, *66*, 634R.
(7) McLuckey, S. A.; Van Berkel, G. J.; Glish, G. L. *J. Am. Soc. Mass Spectrom.* **1992**, *3*, 60.
(8) . McLuckey, S. A.; Habibigoudarzi, S. *J. Am. Chem. Soc.* **1993**, *115*, 12085.
(9) Senko, M. W.; Beu, S. C.; McLafferty, F. W. *Anal. Chem.* **1994**, *66*, 415.
(10) Lee, E. D.; Muck, W.; Henion, J. D.; Covey, T. R. *J. Chromatogr.* **1988**, *458*, 313.
(11) Mann, M.; Meng, C. K.; Fenn, J. B. *Anal. Chem.* **1989**, *61*, 1702. Ferrige, A. G.; Seddon, M. J.; Jarvis, S. *Rapid Commun. Mass Spectrom.* **1991**, *5*, 374. Reinhold: B. B.; Reinhold: V. N. *J. Am. Soc. Mass Spectrom.* **1992**, *3*, 207. Labowsky, M.; Whitehouse, C.; Fenn, J. B. *Rapid Commun. Mass Spectrom.* **1993**, *7*, 71.
(12) Henry, K. D.; McLafferty, F. W. *Org. Mass Spectrom.* **1990**, *25*, 490. Senko, M. W.; Beu, S. C.; McLafferty, F. W. *J. Am. Soc. Mass Spectrom.* **1993**, *4*, 828. Marshall, A. G.; Guan, S. *Rapid Commun. Mass Spectrom.* **1996**, *10*, 1819.
(13) Russell, D. H.; Edmondson, R. D. *J. Mass Spectrom.* **1997**, *32*, 263.
(14) McLuckey, S. A.; Goeringer, D. E. *Anal. Chem.* **1995**, *67*, 2493.
(15) Stephenson, J. L., Jr.; McLuckey, S. A. *J. Am. Chem. Soc.* **1996**, *118*, 7390. Stephenson, J. L., Jr.; McLuckey, S. A. *Anal. Chem.* **1996**, *68*, 4026. McLuckey, S. A.; Stephenson, J. L., Jr.; Asano, K. G. *Anal. Chem.* **1998**, *70*, 1198. Stephenson, J. L., Jr.; McLuckey, S. A. *J. Am. Soc. Mass Spectrom.* **1998**, *9*, 585.

10.1021/ac9809175 CCC: $18.00
Published on Web 12/10/1998

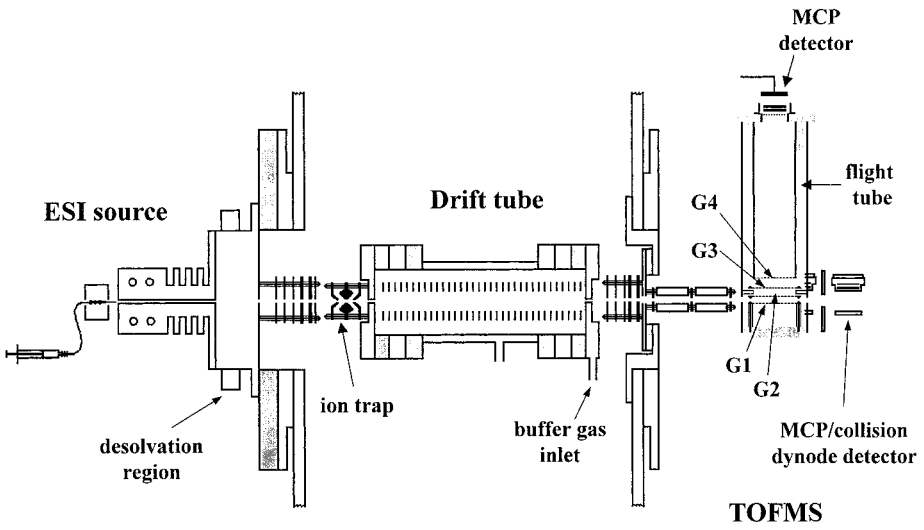

Figure 1. Schematic diagram of the experimental apparatus.

Recently, we have applied ion mobility-based methods for the analysis of a complex mixture of peptides generated by a tryptic digest of ubiquitin.[16] We found that ions were separated primarily by differences in charge state and that this separation led to advantages in resolving peaks with similar m/z ratios but different m and z. Traditionally, ion mobility-MS methods have not been used to characterize *complex* mixtures because of intrinsic methodological limitations. It is typical to discard more than 99% of the continuous ion beam for the pulsed mobility experiment. More ions are filtered away during selection of a single m/z species. The approach that we describe below for the analysis of mixtures differs from conventional ion mobility-MS strategies primarily because of our attention to experimental duty factors. We have developed an ion trap interface to accumulate concentrated ion packets for the pulsed mobility experiment[17] and a nested mobility/time-of-flight MS method[18] that makes it possible to record m/z data for distributions of mobility-separated ions in a single experimental sequence. This paper describes the combined ESI/ion trap/ion mobility/time-of-flight apparatus and experimental approach and presents several example applications that illustrate the following: (1) the ability to reduce spectral congestion in mass spectra of complicated mixtures; (2) the rapid and sensitive nature of the method for analysis of peptide mixtures; and (3) the utility of complementary mobility information for assigning charge states and for distinguishing between different peptide sequences that have virtually identical molecular weights. At this early stage in the development of these methods, it is clear that nested distributions may be influenced by a number of experimental and intrinsic factors, including the following: (1) the concentrations and ionization efficiencies of different analytes in the mixture; (2) the energy used to inject ions into the drift tube; (3) the trapping time used to accumulate ions in the ion trap; and (4) variations in ion conformation with charge state. We have explored a number of these issues and present the results below.

EXPERIMENTAL SECTION

Overview. Ion trap-[19] and ion mobility-MS methods[20,21] have been discussed previously. A schematic diagram of the experimental configuration used in these studies is shown in Figure 1. An overview of the experiment is as follows. A continuous electrospray ion beam is accumulated in the ion trap for ~100 ms. Concentrated packets of ions are injected into the drift tube containing an inert buffer gas. Ions drift through the gas and across the tube under the influence of a weak electric field and are separated by differences in their mobilities. As ions exit the drift tube, they enter the source region of the time-of-flight mass spectrometer. Here, high-voltage, high-frequency pulses synchronous with the initial injection pulse are used to initiate time-of-flight measurements in the mass spectrometer. Because flight times in the evacuated flight tube are much shorter than drift times through the buffer gas, it is possible to record hundreds of mass spectra with respect to each packet of ions that is injected into the drift tube.[18] Flight times at specified drift times are combined to create a three-dimensional data set that contains m/z-resolved ion mobility distributions for all of the electrosprayed ions.

Preparation and ESI of Mixtures. The following peptides and proteins were obtained from Sigma and used without further purification: methionine enkephalin (99%); [Val^5]angiotensin II (>97%); bradykinin (98%); ubiquitin (bovine, 90%); cytochrome *c*

(16) Valentine, S. J. Hoaglund, C. S.; Counterman, A. E.; Reilly, J. P.; Clemmer, D. E. *J. Am. Soc. Mass Spectrom.* **1998**, *9*, 1213.

(17) Hoaglund, C. S.; Valentine, S. J.; Clemmer, D. E. *Anal. Chem.* **1997**, *69*, 4156.

(18) Hoaglund, C. S.; Valentine, S. J.; Sporleder, C. R.; Reilly, J. P.; Clemmer, D. E. *Anal. Chem.* **1998**, *70*, 2236.

(19) March, R.; Huges, R.; *Quadrupole Storage Mass Spectrometry*, Wiley: New York, 1989. Cooks, R. G.; Kaiser, R. E., Jr. *Acc. Chem. Res.* **1990**, *23*, 213. Glish, G. L.; McLuckey, S. A. *Int. J. Mass Spectrom. Ion Processes* **1991**, *106*, 1. March, R. E. *J. Mass Spectrom.* **1997**, *32*, 351.

(20) Hagen, D. F. *Anal. Chem.* **1979**, *51*, 870. Tou, J. C.; Boggs, G. U. *Anal. Chem.* **1976**, *48*, 1351. St. Louis, R. H.; Hill, H. H. *Crit Rev. Anal. Chem.* **1990**, *21*, 321. Hill, H. H.; Siems, W. F.; St. Louis, R. H.; McMinn, D. G. *Anal. Chem.* **1990**, *62*, 1201A. von Helden, G.; Hsu, M.-T.; Kemper, P. R.; Bowers, M. T. *J. Chem. Phys.* **1991**, *95*, 3835. Karpas, Z.; Stimac, Rappaport, Z. *Int. J. Mass Spectrom. Ion Processes* **1988**, *83*, 163. Jarrold, M. F. *J. Phys. Chem.* **1995**, *99*, 11.

(21) For recent reviews of ion mobility studies of biomolecules, see: Clemmer, D. E.; Jarrold, M. F. *J. Mass Spectrom.* **1997**, *32*, 577. Liu, Y.; Valentine, S. J.; Counterman, A. E.; Hoaglund, C. S.; Clemmer, D. E. *Anal. Chem.* **1997**, *69*, 728A.

(horse heart, >99%); and myoglobin (99%). For studies involving known mixtures, stock solutions were prepared and combined in appropriate concentrations. Peptide mixtures from tryptic digests of cytochrome *c* and myoglobin were generated by addition of 150 μL of a 0.2 mg/mL trypsin (Sigma, sequencing grade) solution in 0.2 M ammonium bicarbonate (EM Science) to 0.5 mL of a 20 mg/mL solution of each protein. After incubation for 20 h at 37 °C, the trypsin was filtered from the digest using a microconcentrator (Microcon 10, Amicon, Inc.) and the peptides that remained were lyophilized.

Positively charged (protonated) ions were formed by electrospraying solutions containing 5×10^{-7}–4×10^{-5} M peptide (or 0.5 mg/mL tryptic digest) in 49:49:2 (% vol) water/acetonitrile/acetic acid. The ESI needle was biased +3200 V relative to the entrance of the desolvation region. Typical solution flow rates were 0.05–0.10 mL/h. Solutions were electrosprayed at atmospheric pressures into a variable-temperature differentially pumped desolvation region. The desolvation region is 5 cm long and is operated at a pressure of 1–10 Torr. A fraction of the ions exit the differentially pumped cavity through a 0.010-cm-diameter orifice and enter the main chamber of the instrument.

Ion Trap Interface. Ions that exit the source are focused into a low-energy ion beam and guided into an ion trap that accumulates the continuous beam between pulses. The experimental arrangement used here is similar to one used for ESI/time-of-flight MS experiments[22] and identical to the interface that we developed previously for ESI/ion mobility experiments.[22] Briefly, the trap (R. M. Jordan model C-1251) consists of two end-cap electrodes and a center ring electrode that are isolated by ceramic guard rings. Ions continuously enter the trap (except during the short ejection pulse) through a 0.32-cm-diameter aperture where they experience a 1.1-MHz rf field applied to the ring electrode. These studies use rf fields ranging from 2000 to 2800 V (peak-to-peak) depending on the m/z ratios of the ions that are being trapped. The pressure inside the trap ($\sim 10^{-4}$–10^{-3} Torr) is supplied from buffer gas that leaks out of the entrance of the drift tube and ambient gas pressure in the main chamber. Ions inside the trap become confined to a small volume in the center that is aligned with the drift tube entrance aperture. Ions are ejected through a 0.16-cm-diameter exit aperture by turning off the rf field and supplying a short (0.5 μs) dc pulse (−100 to −200 V) to the exit end cap. Ejected ions enter the drift tube entrance aperture without additional focusing.

The trap is biased to within a few volts of the exit plate of the high-pressure source. This voltage is key for trapping ions and was maintained to within 30 V of the source plate in all of the studies reported here. Ion injection energies into the drift tube are defined by the voltage difference between the trap and the entrance plate of the drift tube as well as the charge state of the ion. Extensive studies (carried out previously[17]) as a function of ejection pulse voltage and time between turning off the rf field and applying the pulse (from 0.2 to ~4 μs) showed no significant effect on the ion signal.

Injected-Ion Drift Tube. The injected-ion drift tube is 40.4 cm long with 0.008-cm-diameter entrance and exit apertures. Data were recorded using ~2–3 Torr of 300 K He buffer gas and applied drift fields of 8–10 V cm^{-1}. Entrance and exit plates are electrically isolated from the drift tube body with ceramic spacers machined from Mycalex (McMaster Carr). A uniform electric field along the drift axis is created by 30 equally spaced 0.025-cm-thick BeCu rings that are connected by a series of 5.00-MΩ high-vacuum resistors (KDI Electronics, ±1%).

Mass Spectrometer. When ions exit the drift tube, they enter an einzel/dc-quadrupole lens system that is designed to focus the ion beam into the shape of a ribbon. Ions travel ~25 cm across this focusing region and exit through a slit (0.16 × 1.27 cm) into the extraction region of the TOF MS instrument. Four grids (labeled G1–G4 in Figure 1) are used to extract and focus ions to the TOF detector. The TOF measurement is initiated by a voltage pulse (3 μs, +2220 V) supplied by a high-voltage pulser (Directed Energy Inc., model GRX-3.OK-H) to the grid labeled G1. The G2, G3, and G4 grids were maintained at potentials of −50, −1210, and −5730 V (the flight tube potential), as calculated by a space- and velocity-focusing algorithm that takes into account the geometry of the instrument as described previously.[23] The field-free region of the flight tube is 17.5 cm long. Ions are detected by a pair of microchannel plates mounted directly to the back of the flight tube.

An additional detector that is collinear with the drift tube is used initially to focus the ion beam. For ion focusing, ions pass through G1 and G2 of the TOF extraction region and are accelerated and focused onto a collision dynode/microchannel plate detection system. Both detectors and the TOF instrument are housed in a separate differentially pumped chamber; the typical pressure during experiments is $\sim 1 \times 10^{-6}$ Torr.

Ion Mobility and TOF Considerations. We refer to the term *drift time* as the time required for ions to travel through the high-pressure drift tube as given by[24]

$$t_D = L/E_D K \tag{1}$$

where K is the mobility of the ions, L is the length of the drift tube, and E_D is the applied drift field. The term *flight time* refers to the time required for ions that have been accelerated to a desired kinetic energy in a vacuum to travel through the field-free region of the mass spectrometer. The flight time is

$$t_F = l(m/2zE_{TOF})^{1/2} \tag{2}$$

where l is the length of the field-free region, m is the ion mass, z is the ion charge state, and E_{TOF} is the kinetic energy of the ions.

The arrival time of a packet of ions at the detector is a composite of the drift time, flight time, and time required to travel through other portions of the instrument. It is necessary to account for the flight time and a small correction associated with transport of the ions from the exit of the drift tube to the entrance of the time-of-flight region in determining t_D. The correction time is small (80–140 μs) compared to the 2–7-ms drift times in these experiments. The reduced mobility for each ion is determined from[24]

(22) Michael, S. M.; Chien, M.; Lubman, D. M. *Rev. Sci. Instrum.* **1992**, *63*, 4277. Michael, S. M.; Chien, B. M.; Lubman, D. M. *Anal. Chem.* **1993**, *65*, 2614. Quian, M. G.; Lubman, D. M. *Anal. Chem.* **1995**, *67*, 234A.

(23) Colby, S. M.; Reilly, J. P. *Anal. Chem.* **1996**, *68*, 1419.

(24) Mason, E. A.; McDaniel, E. W. *Transport Properties of Ions in Gases*; Wiley: New York, 1988.

$$K_0 = \frac{L}{t_D E}\frac{P}{760}\frac{273.2}{T} \quad (3)$$

where the measured parameters t_D, E, L, P, and T correspond to the average drift time, the electric field strength, the drift tube length, buffer gas pressure (in Torr), and temperature, respectively. Experimental collision cross sections are obtained directly from the ion mobility distributions by the relation[21]

$$\Omega = \frac{(18\pi)^{1/2}}{16}\frac{ze}{(k_b T)^{1/2}}\left[\frac{1}{m_I}+\frac{1}{m_B}\right]^{1/2}\frac{t_D E}{L}\frac{760}{P}\frac{T}{273.2}\frac{1}{N} \quad (4)$$

that contains the mobility expression. The other terms are as follows: ze, the ion's charge; N, the neutral number density; k_b, Boltzmann's constant; and m_I and m_B, the masses of the ion and buffer gas, respectively. All of the parameters E_D, L, P, T, and t_D can be precisely measured. Thus, the reproducibility of measured cross sections is excellent. Ion energies in the drift tube are determined by E_D/N. The present experiments were carried out at low E_D/N, where mobilities are independent of the applied drift field and drift velocities are small compared with the thermal velocity of the buffer gas. Under these conditions, ions are not expected to align in the drift tube and we assume that collision cross sections correspond to an average of all possible orientations.

Acquisition of Nested Drift (Flight) Time Data. Simultaneous measurements of mobilities and m/z ratios are feasible because flight times are much shorter than drift times. This allows flight times of the different m/z ions to be measured within individual time windows of the ion mobility spectrum. We refer to this as a nested measurement and denote drift and flight times as $t_D(t_F)$, (in units of ms and μs, respectively).[18] Acquisition of $t_D(t_F)$ data is carried out as follows. The initial injection pulse activates a programmable delay generator (PDG, Lecroy 4222) that triggers the high-voltage TOF pulser at specified delay times. In these experiments, an accumulation of 256 windows (each 50 or 100 μs in duration) creates the ion mobility distribution. Flight times in the mass spectrometer are recorded using a time-to-digital converter (TDC, Lecroy 4208) that is also initiated by the PDG pulse sequence. The TDC records the time that ions reach the detector during the first 32 μs of the 100-μs drift time window with 1-ns resolution. The instrumental electronics and data acquisition system, including the initial injection pulse, PDG pulse sequence, TDC, and high-voltage TOF pulser are synchronized by an interface and under computer control. Peak identification and integration programs were written in-house. Three-dimensional plots of the data were created using the MATLAB software.[25]

Experimental Duty Cycle. We define the overall experimental duty cycle as the fraction of the continuous ion signal passing through the drift tube that is utilized during nested drift (flight) time measurements. The total continuous ion signal can be measured directly using the on-axis collision dynode/microchannel plate detector. For 0.5-μs ejection pulses and trapping times in excess of 50 ms, one calculates that the duty cycle approaches 100% for injection of ions from the ion trap into the drift tube. In previous studies[17] of negatively charged maltotetraose ions, we compared signal-to-noise (S/N) ratios for spectra recorded with and without the ion trap; dramatic improvements in S/N ratios indicated that from 60 to 100% of ions are trapped and can be used for experiments. Similar studies of electrosprayed peptides and proteins carried out in the present instrument indicate that ~70−100% of the ions are utilized for experiments. These values depend on the injection voltages that are used; trapping efficiencies decrease slightly with increasing injection voltage due to leakage of ions from the trap. For the peptide and protein systems described below, we are typically able to utilize more than ~90% of the ion signal when injection voltages below 100 V are used.

The duty cycle associated with the time-of-flight detection depends on the time required for ions to travel into the pulse grid region and the experimental repetition rate (limited by the highest m/z ion). When the time between high-voltage pulses is similar to the time required for ions to fill the source region, then duty cycles should be high. If the time between pulses is significantly longer than the time required for ions to fill this region, then ions pass through the source region and are lost. We have estimated the duty cycle in this region by comparing signal intensities using the on-axis detector (with no mass analysis) to those when ions are dispersed in the off-axis mass spectrometer. From integrated ion intensities for data recorded at the different detectors for identical time periods, we estimate that ~5−10% of ions are detected at the off-axis detector. Considerations of repetition rates and estimates of the times required to fill the source region indicate that the majority of ions are lost because they pass through the source region between pulses of the source grid; ions may also miss the off-axis detector. Efforts to improve the experimental duty cycle in this region are currently underway.

Detection limits were determined from studies that used mixtures of known composition. For a variety of simple peptide and protein mixtures (containing two to five components such as bradykinin, [Val^5]angiotensin II, methionine enkephalin, ubiquitin, and cytochrome *c*), all components can be detected in a few seconds (with mobility separation and m/z dispersion) at detection limits (S/N > 3) of ~0.5−3.0 pmol of consumed sample. This range is similar to the 1.3-pmol detection limit that we reported previously for deprotonated maltotetraose ions for mobility measurements without m/z analysis.[17] As shown below, these detection limits are sufficient to allow rapid analysis of complex biomolecular mixtures.

RESULTS AND DISCUSSION

Separation of $[M + H]^+$ and $[M + 2H]^{2+}$ Charge-State Families in Tryptic Fragment Mixtures. Figure 2 shows a nested drift (flight) time data set for a mixture of peptides generated from a tryptic digest of cytochrome *c*. These data are shown as a two-dimensional contour plot; individual axes corresponding to the time-of-flight mass spectrum (left) and ion mobility distribution (bottom) are also displayed. A striking feature of this plot is that most of the peaks fall into one of two ion families: high- and low-mobility ions that arrive at short and long times, respectively, for a given m/z. The basis for separation of ions into these families can be understood by assigning several peaks. Peaks 1w at 2.63 ms (3.284 μs, $m/z = 389.0$), 1o at 3.45 ms (4.098 μs, $m/z = 605.8$), and 1i at 4.23 ms (4.654 μs, $m/z = 781.5$) in the

(25) MATLAB Version 4, The Math Works Inc.: Natick, MA, 1997.

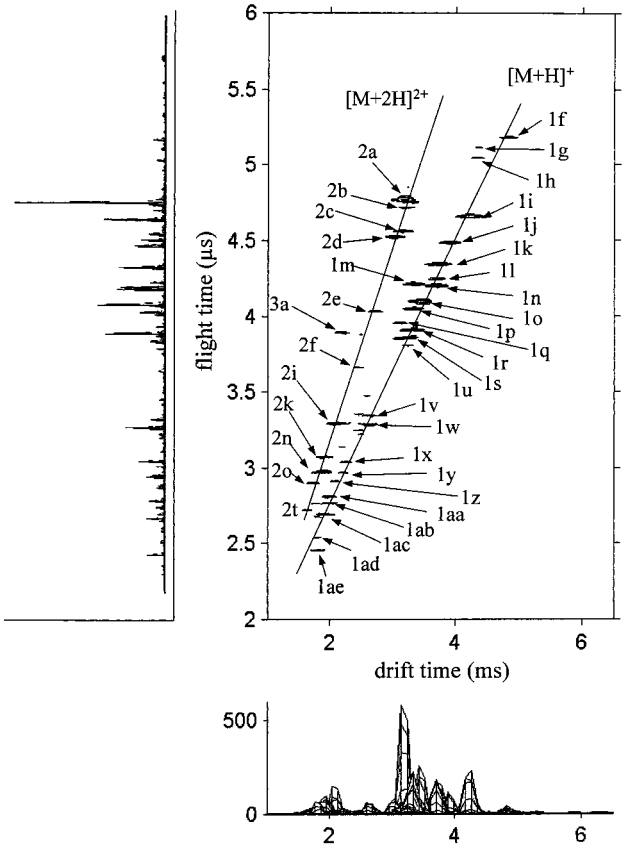

Figure 2. Contour plots of nested drift time (bottom) and flight time (left) data for a mixture of peptide ions that were formed by direct electrospray of a tryptic digest of cytochrome *c*. The resolving power along the flight time axis is typically 300 ($m/\Delta m$ of a peak for a singly charged ion where Δm is determined at half-maximum). The drift time axis has been scaled to a helium pressure of 2.000 Torr. Ions were trapped for 150 ms prior to injection at 90 V. The contours are shown on a 30-point scale; this removes all features that contain fewer than 30 ion counts. The peak labels are described in the text and flight times, drift times, and assignments of peaks are given in Table 1. Projections of the data along the bottom and left axes show ion mobility and time-of-flight distributions, respectively.

low-mobility family can be assigned to the singly protonated ions of AGIK (mol wt = 387.5), GITWK (mol wt = 603.7), and MIFAGIK (mol wt = 779.0), respectively, that are expected from the tryptic digest. Peaks 2n at 1.86 ms (2.970 μs, $m/z = 318.2$), 2i at 2.08 ms (3.291 μs, $m/z = 390.7$), and 2d at 3.04 ms (4.520 μs, $m/z = 737.0$) in the high-mobility family can be assigned to the doubly protonated peptides IFVQK (mol wt = 633.8), MIFAGIK (mol wt = 779.0), and TGQAPGFTYTDANK (mol wt = 1470.6), respectively. The summary of assignments given in Table 1 indicates that the low- and high-mobility families correspond to $[M + H]^+$ and $[M + 2H]^{2+}$ ions, respectively. An additional peak labeled 3a and discussed more below also corresponds to a tryptic fragment. In all, we assign 18 peaks to tryptic digest products, including one fragment ($[EDLIAY + H]^+$) that probably results from chymotryptic activity, as well as $[KK + H]^+$, $[GKK + H]^+$, $[KTER + 2H]^{2+}$ and $[KATNE + H]^+$ (at the C-terminal end, Table 1) that result from incomplete digestion. This provides an extensive map of the protein that spans all but two regions of the sequence: $G^{34}LFGR^{38}$ and $Ac\text{-}G^{1}DVEK^{5}$. Fourteen peaks (Table 1) cannot be immediately assigned to expected fragments. Most of these peaks are small in comparison to the tryptic peptide peaks; they may arise from sample impurities or fragmentation of peptide ions. The latter possibility is discussed in detail below.

The observation of $[M + H]^+$ and $[M + 2H]^{2+}$ charge state families for cytochrome *c* fragments is consistent with our recent findings for ubiquitin[16] and digests of seven other proteins. Ion mobility-based separation of these charge states into families can be understood by considering that the drift force experienced by doubly charged ions is twice that experienced by singly charged ions. The observation of only +1 and +2 charge states is expected because trypsin cleaves proteins after basic residues.[26] Peptides resulting from complete digestion should have two protonatable sites: the basic amino acid on the C-terminal end and the N-terminal amino group. Higher charge states may be observed for a number of reasons, including incomplete digestion (as is sometimes the case for regions of the sequence having neighboring basic residues)[26] and the presence of disulfide-bonded regions or an ionizable heme group in the peptide sequence. In several cases, only one of the two possible charge states is observed. Often small fragments are only observed in the +1 charge state. We presume that the +2 state is unfavorable because the amino terminus (which has a relatively low basicity compared with lysine, arginine, and histidine residues[27]) cannot stabilize a second proton that is in close proximity to a protonated lysine or arginine residue; it is possible that the abundances of small +1 or +2 peptides are also influenced by solution properties or other factors that occur in the final stages of ion formation. Often singly protonated states of large peptides (i.e., those with more than ~16 residues) are not observed.[28] Fragments associated with chymotryptic activity (e.g., peak 1j in Figure 2) usually have only a single protonatable site (the N-terminal amino group).

Although the majority of assignments given in Table 1 can be made solely on the time-of-flight measurement, clear advantages of the mobility-based separation are apparent. Separation of ions into charge-state families reduces congestion of the mass spectral axis, and the additional mobility information corroborates the assignment of charge state in the m/z measurement. Second, for several ions, separation by charge state is useful in resolving $[M + H]^+$ and $[M + 2H]^{2+}$ ions with similar m/z ratios. Peaks 1w at 3.284 μs ($m/z = 389.0$) and 2i at 3.291 μs ($m/z = 390.7$) as well as peaks 1y at 2.968 μs ($m/z = 317.7$) and 2n at 2.970 μs ($m/z = 318.2$) are easily resolved and identified when they are first separated by differences in their mobilities.

Rapid Data Acquisition. Figure 3 shows contour plots of a distribution of cytochrome *c* fragments when data are acquired for 60 s and 6 min. Peak assignments were taken from Table 1. In 60 s, it is possible to identify 15 of the 22 peaks that we have attributed to tryptic fragments (Figure 2). In 6 min, 21 peaks can be assigned. The only missing peak corresponds to the $[EDLIAY\text{-}LK + 2H]^{2+}$ ion (2f, a small peak in Figure 2). Rapid data

(26) Findlay, J. B. C., Gelsow, M. J., Eds. *Protein Sequencing: A Practical Approach*; IRL Press: Oxford, 1989; p 43.

(27) Protonation of the N-terminus has been investigated extensively for a series of small polyglycine oligomers (Gly_1-Gly_{10}). The proton affinities increase with increasing size due to stabilizing effects from the presence of additional residues. For discussions, see: Wu, Z.; Fenselau, C. *J. Am. Soc. Mass Spectrom.* **1992**, *3*, 863; Zhang, K.; Zimmerman, D. M.; Chung-Phillips, A.; Cassady, C. J. *J. Am. Chem. Soc.* **1993**, *115*, 10812; Wu, J.; Lebrilla, C. B. *J. Am. Chem. Soc.* **1993**, *115*, 3270.

(28) It is possible that our detection conditions are less sensitive to high-m/z ions.

Table 1. Flight Times, Masses, and Assignments of Tryptic Digest Peptides of Cytochrome *c*[a]

$[M + H]^+$ family		$[M + 2H]^{2+}$ family					
peak label	t_f (mass)[b]	peak label	t_f (mass)[b]	neutral mass [M][c]	assignment[d]	calcd mol wt[e]	fragment position[f]
1ae	2.455 (217.4)			216.4			
1ad	2.539 (232.5)			231.5			
1ac	2.692 (261.4)			260.4	NK or GGK	260.3	54−55 or 23−25
1ab	2.765 (275.8)			274.8	KK	274.4	87−88
1aa	2.808 (284.5)			283.5	HK	283.3	26−27
1z	2.911 (305.7)			304.7			
1y	2.968 (317.7)			316.7			
1x	3.037 (332.8)			331.8	GKK	331.4	6−8
1w	3.284 (389.0)			388.0	AGIK	387.5	
1v	3.342 (402.9)			401.9			
1u	3.806 (522.5)			521.5			
		2t	2.721 (534.3)	532.3	KTER	532.6	88−91
1s	3.856 (536.5)			535.5			
1r	3.907 (550.7)			549.7			
1q	3.952 (563.5)			562.5	KATNE	561.6	100−104
1p	4.046 (590.6)			589.6			
1o	4.098 (605.8)	**2o**	2.898 (605.8)	604.3	GITWK	603.7	56−60
1n	4.199 (636.0)	**2n**	2.970 (636.3)	634.7	IFVQK	633.8	9−13
1m	4.211 (639.6)			638.6	TGPNLH	637.6	28−33
1l	4.244 (649.8)			648.8			
1k	4.342 (680.3)	**2k**	3.070 (679.8)	678.6	YIPGTK	677.8	74−79
1j	4.483 (725.2)			724.2	EDLIAY	722.7	92−97
1i	4.654 (781.5)	**2i**	3.291 (781.4)	779.9	MIFAGIK	779.0	80−86
1h	5.042 (916.9)			915.9			
1g	5.114 (943.4)			942.4			
1f	5.179 (967.6)	**2f**	3.661 (966.8)	965.7	EDLIAYLK	964.1	92−99
		2e	4.030 (1172.0)	1170.0			
		2d	4.520 (1474.1)	1472.1	TGQAPGFTYTDANK	1470.6	40−53
		2c	4.559 (1499.4)	1497.4	EETLMEYLENPK	1495.7	61−72
		2b	4.713 (1602.7)	1600.7			
		2a	4.764 (1637.6)	1635.6	CAQCHTVEK (heme)[g]	1636.4	14−22 (heme)

[a] Peaks assigned in Figure 2. [b] Measured flight times (t_f) in μs. Masses for $[M + H]^+$ and $[M + 2H]^{2+}$ species from tryptic digests are given in parentheses. Average masses were derived from the centers of flight time peaks by using a calibration that was determined by electrospraying known solution mixtures (usually bradykinin and angiotensin or polyalanines). The accuracy of these results can be accessed by comparing the experimental masses to calculated values that are also given. Estimated uncertainties in masses are ±0.5 u. [c] Mass of the neutral peptide determined from nested data. In cases where both the $[M + H]^+$ and $[M + 2H]^{2+}$ ions were observed, the mass is an average of both measurements, after correction for the mass shift associated with additional hydrogens. [d] Sequences that are expected for the complete tryptic digest of horse heart cytochrome *c*, having the sequence: Ac-GDVEK∫ GK∫ K∫ IFVQK∫ CAQCHTVEK∫ GGK∫ HK∫ TGPNLHGLFGR∫ K∫ TGQAPGFTYTDANK∫ NK∫-GITWK∫ EETLMEYLENPK∫ K∫ YIPGTK∫ M IFAGIK∫ K∫ K∫ TE R∫ EDLIAYLK∫ K∫ ATNE. The heme is covalently bound to Cys^{14} and Cys^{17}. [e] Molecular weights correspond to the isotopic average for each peptide. [f] Position of the peptide fragment in the sequence. [g] The assignment of peak 2a comes from a detailed molecular modeling analysis of peak 3a in Figure 2. See text.

acquisition raises an intriguing possibility of using the nested approach as a detection method for liquid chromatography. The reduced spectral congestion and charge-state assignment may facilitate analysis of tremendously complex mixtures; as shown below, combined with molecular modeling this approach can allow unambiguous distinction between components that cannot be resolved on the basis of differences in m/z ratios alone. Efforts to decrease data acquisition times to a few seconds are currently underway in our laboratory.

Combined Molecular Modeling and Experiment for Distinguishing between Peptides with Nearly Identical Molecular Weights. Distinguishing between two ions with similar m/z but different z can be accomplished by mobility-based determination of charge-state family or by high-resolution MS measurements of isotopic spacing. Unambiguous assignment of peaks becomes more challenging when two ions having nearly identical molecular weights also have the same charge. This case arises for the $I^9FVQKCAQCHTVEK^{22}$ (mol wt = 1633.820) and heme-$C^{14}AQCHTVEK^{22}$ (mol wt = 1633.615) fragments that possibly exist in the cytochrome *c* digest. Both fragments are consistent with the flight time measured for peak 2a in the $[M + 2H]^{2+}$ family (Figure 2). Russell and Edmondson assigned an analogous +1 ion peak in a matrix-assisted laser desorption/ionization spectrum of a tryptic digest mixture to the heme-$C^{14}AQCHTVEK^{22}$ peptide based on high-accuracy high-resolution data.[13] Here, we illustrate the application of ion mobility measurements combined with molecular modeling to assignment of sequences. This approach requires that sequences be known. In the present system, both sequences are somewhat unique as tryptic fragments because they have three possible charge sites: the K^{13}, K^{22}, and N-terminal amino group in the $I^9FVQKCAQCHTVEK^{22}$ peptide and the K^{22}, N-terminal amino group and ionizable heme in the heme-C^{14}-$AQCHTVEK^{22}$ peptide. Indeed, peak 3a at 2.17 ms (3.890 μs, m/z = 545.9) arrives at shorter drift times than is expected for the $[M + 2H]^{2+}$ family, consistent with formation of an $[M + 3H]^{3+}$ ion.

We proceed by modeling each of the two triply charged peptide candidates ($[IFVQKCAQCHTVEK + 3H]^{3+}$ and [heme-$CAQCHTVEK + 2H]^{3+}$) and comparing the cross sections that are obtained from an array of conformers generated for each peptide sequence to the experimental data. Trial structures were obtained by using the Insight II molecular modeling software

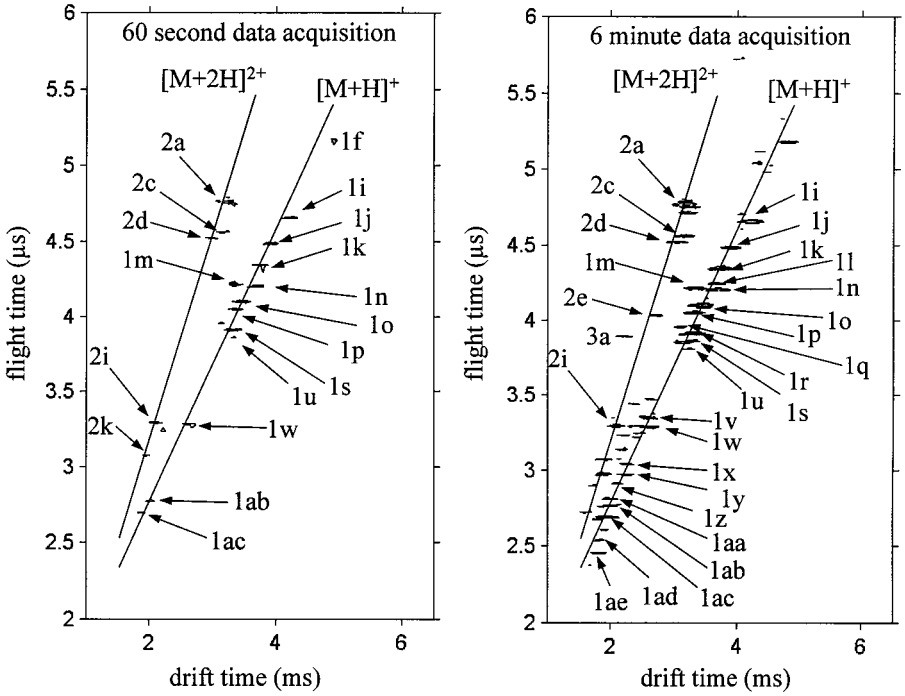

Figure 3. Contour plots of nested data for the cytochrome *c* digest shown in Figure 2 using data acquisition times of 60 s and 6 min.

using the ESFF force field.[29] The force field used a dielectric constant of 1.0 for the surrounding media; thus, these are in vacuo conformations.[30] For each sequence, 100 different conformers were generated by a simulated annealing approach. The temperature was increased to 1000 K over 2 ps, equilibrated for 2 ps, and then cooled over 1 ps to 300 K. Cross sections for individual conformers were estimated by calculating the average projection[31] when the coordinates are rotated through all possible orientations. For the purposes of distinguishing between the I^{9}-FVQKCAQCHTVEK[22] and heme-C^{14}AQCHTVEK[22] peptides, it is unnecessary to determine the absolute lowest energy structure; we assume that the ions' conformations fluctuate as they travel the drift tube. The annealing procedure is employed to gain an understanding of probable conformations and their energetic accessibility. Determination of actual populations and lifetimes of different conformations that are accessed by the ion at 300 K as it travels through the drift tube is a substantially more challenging problem.

Figure 4 shows a plot of cross sections and energies for each of the conformers obtained in the simulated annealing study. From the comparison of these values with the 336 ± 8 Å^2 cross section determined for peak 3a in Figure 2, we have assigned this feature to the [heme-CAQCHTVEK +2H]$^{3+}$. Simulated annealing of this peptide yields some conformations that have cross sections that are in agreement with the experimental result; the average of all values is 359 ± 10 Å^2, 7% above the experimental value. Calculated cross sections for all of the modeled conformations of [IFVQK-CAQCHTVEK + 3H]$^{3+}$ are substantially larger than experiment. The average value, 427 ± 9 Å^2, is 27% greater, far outside the values required for any reasonable assignment. The insets in Figure 4 show typical conformers that were obtained from the simulated annealing procedure and provide an understanding of the structural differences between the two possible sequences. The triply protonated [IFVQKCAQCHTVEK + 3H]$^{3+}$ has an extended conformation in order to minimize Coulombic repulsion between the three rather evenly spaced protonated sites. The presence of the heme group allows the [heme-CAQCHTVEK + 2H]$^{3+}$ ion to adopt more compact conformations. In the end, our assignment agrees with the assignment made by Russell and Edmondson.[13]

Influence of Experimental Parameters on Nested Distributions. Having shown that it is possible to rapidly acquire mobility-separated mass spectra for complex mixtures, it is important to address how various experimental factors influence the nested distributions that are observed. In initial studies, we examined 10 individual peptide or protein systems and several electrosprayed mixtures. The results described below were observed in most of the systems that were examined. Factors such as analyte concentration, solution pH,[32] solvent composition and temperature,[33,34] and capillary temperature[35] are known to influ-

(29) Insight II.; BIOSYM/MSI: San Diego, CA, 1995.

(30) The ESFF force field was chosen because metal atoms can be accommodated. Trial conformers calculated for [IFVQKCAQCHTVEK + 3H]$^{3+}$ have cross sections that are similar to those obtained using ESFF.

(31) The accuracy of methods for calculating cross sections for very large molecules is a topic that is currently being investigated. Bowers and coworkers have developed a method for determining empirical hard-sphere impact parameters based on temperature-dependent mobilities for ions with known structures. For a discussion, see: von Helden, G.; Wyttenbach, T.; Bowers, M. T. *Int. J. Mass Spectrom. Ion Processes* **1995**, *146/147*, 349. We utilize this method here. The following Lennard-Jones impact parameters for collisions of He with atoms of the peptide were used: 2.38 for hydrogen; 3.02 for carbon, nitrogen, and oxygen. A value of 3.2 was used for sulfur. These values are taken from a discussion in the appendix of: Wyttenbach, T.; Bushnell, J. E.; Bowers, M. T. *J. Am. Chem. Soc.* **1998**, *120*, 5098. A more rigorous (albeit time-consuming) approach involving trajectory calculations has also been developed: Mesleh, M. F.; Hunter, J. M.; Shvartsburg, A. A.; Schatz, G. C.; Jarrold, M. F. *J. Phys. Chem.* **1996**, *100*, 16082.

(32) Chowdhury, S. K.; Katta, V.; Chait, B. T. *J. Am. Chem. Soc.* **1990**, *112*, 9012.

(33) Loo, J. A.; Loo, R. R. O.; Udseth, H. R.; Edmonds, C. G.; Smith, R. D. *Rapid Commun. Mass Spectrom.* **1991**, *5*, 101.

(34) Mirza, U. A.; Cohen, S. L.; Chait, B. T. *Anal. Chem.* **1993**, *65*, 1.

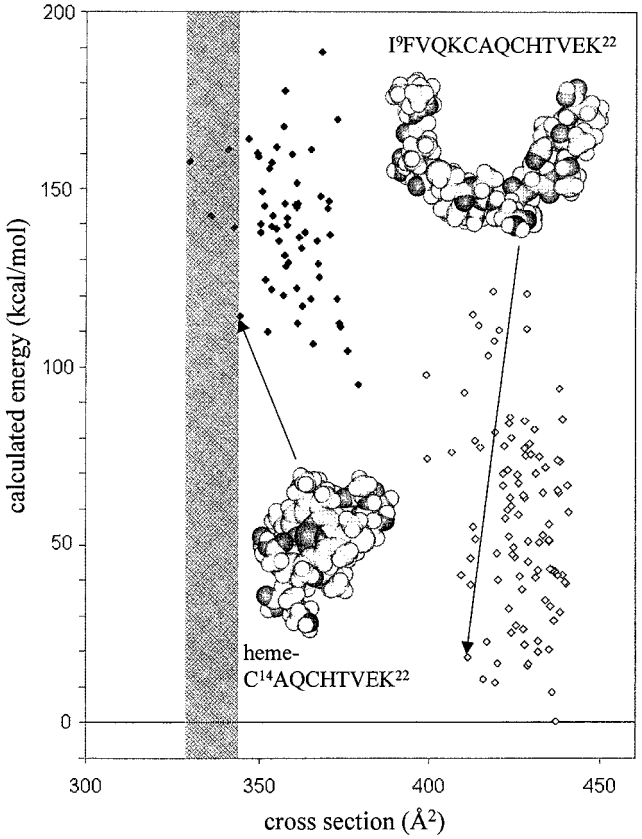

Figure 4. Calculated cross sections and energies for 100 conformations of [heme-CAQCHTVEK + 2H]$^{3+}$ (solid diamonds) and [IFVQKCAQCHTVEK + 3H]$^{3+}$ (open diamonds) that were generated by a simulated annealing/molecular modeling procedure (see text). The energy axis has been defined relative to the lowest energy structure that was found in both sequences. These results are compared with an experimental cross section of 336 ± 8 Å^2 derived for peak 3a (m/z = 545.9), shown as the shaded region. Although the experimental m/z ratio is consistent with both m/z = 545.2 (calculated for [heme-CAQCHTVEK + 2H]$^{3+}$) and 545.6 (calculated for [IFVQKCAQCHTVEK + 3H]$^{3+}$), the molecular modeling results show that peak 3a must be due to the [heme-CAQCHTVEK + 2H]$^{3+}$ ion. Example structures of each sequence are also shown.

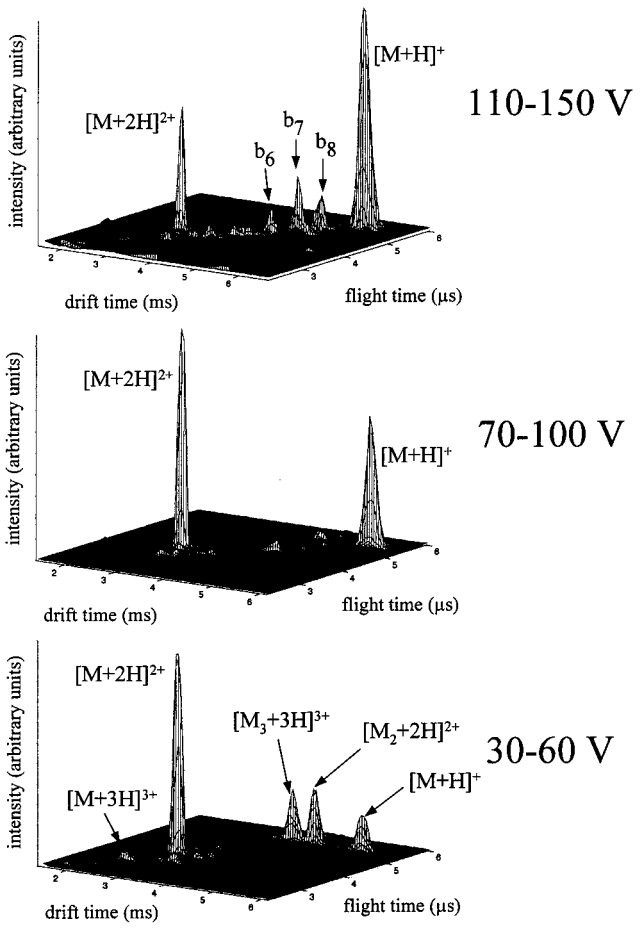

Figure 5. Three-dimensional plots of drift time, flight time, and ion intensity for distributions of electrosprayed bradykinin ions as a function of injection voltage. The data shown are representative of distributions that are observed when ions are injected using 30−60, 70−100, and 110−150 V. The drift time axis has been scaled to a helium pressure of 2.000 Torr.

ence charge-state distributions. Nested distributions for individual peptides are especially sensitive to analyte concentration and injection voltage. Small peptides such as bradykinin (nine residues) and angiotensin II (eight residues) favor the +2 and +1 charge states at high analyte concentrations (5×10^{-5}−8×10^{-4} M); the +2 and +3 states are favored at concentrations below 5×10^{-5} M.

An example of the influence of injection voltage upon nested data is shown in Figure 5 for electrosprayed bradykinin ions that were injected at low (30−60 V), medium (70−100 V), and high (110−150 V) injection voltages. All three data sets show a large peak at 2.49 (3.84) which corresponds to the [M + 2H]$^{2+}$ ion (m/z = 531) having Ω = 246 Å^2, in agreement with previous measurements.[36] A much smaller feature at 2.06 (3.15) is assigned to [M + 3H]$^{3+}$. At low injection voltages, peaks at 3.49 (5.42), 3.96 (5.42), and 4.90 (5.42) have m/z =1061 and correspond to the [M + H]$^+$ monomer, [M_2 + 2H]$^{2+}$ dimer, and [M_3 + 3H]$^{3+}$ trimer ions, respectively, as assigned previously.[36] When the injection voltage is increased (70−100 V), the fractions of [M_2 + 2H]$^{2+}$ and [M_3 + 3H]$^{3+}$ ions decrease; the corresponding fraction of [M + H]$^+$ monomer ion increases, consistent with collision-induced dissociation of the multiply charged multimers. At higher injection voltages (110−150 V), the fraction of +2 ions decreases and a series of peaks at 3.84 (4.44), 4.11 (4.73), and 4.38 (5.01) corresponding to the b_6, b_7, and b_8 fragments, respectively, is observed. Because no initial mass filter is used, we cannot unambiguously account for the origin of these products; however, it is likely that dissociation of +2 ions yields these fragments. A notable feature in these (and other) data is that at high injection energies the magnitude of the [M + 2H]$^{2+}$ peak becomes substantially smaller than the [M + H]$^+$ peak. In many cases, this decrease is larger than can be explained solely by dissociative

(35) LeBlanc, J. C. Y.; Beuchemin, D.; Siu, K. W. M.; Guevremont, R.; Berman, S. S. *Org. Mass Spectrom.* **1991**, *26*, 831. Rockwood, A. S.; Busman, M.; Udseth, H. R.; Smith, R. D. *Rapid Commun. Mass Spectrom.* **1991**, *5*, 582. Goldstein, G.; Scheid, M.; Hammerling, U.; Boyse, E. A.; Schlesinger, D. H.; Niall, H. D. *Proc. Natl. Acad. Sci. U.S.A.* **1975**, *72*, 11.

(36) Counterman, A. E.; Valentine, S. J.; Srebalus, C. A.; Henderson, S. C.; Hoaglund, C. S.; Clemmer, D. E. *J. Am. Soc. Mass Spectrom.* **1998**, *9*, 743.

(37) The proton affinity of He is 42.5 kcal/mol, as given by: Lias, S. G.; Bartmess, J. E.; Liebman, J. F.; Holmes, J. L.; Levin, R. D.; Mallard, W. G. *J. Phys. Chem. Ref Data* **1988**, *14* (Suppl. 1), 1.

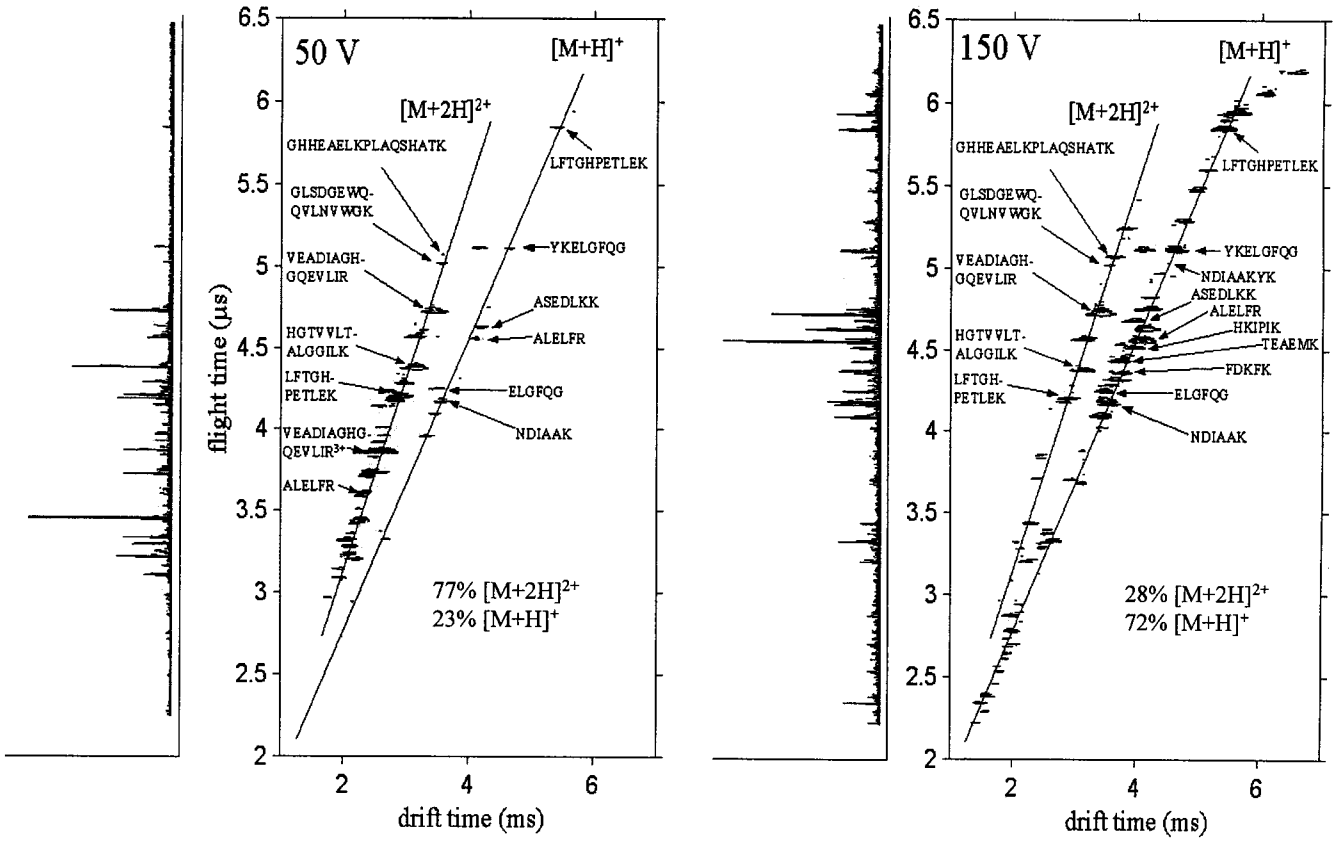

Figure 6. Contour plots of nested data for a mixture of peptides from a digest of myoglobin when ions are injected into the drift tube at 50 and 150 V. Projected mass spectra are shown to the left of each contour plot. Other experimental conditions were the same as those shown in Figure 2.

loss of $[M + 2H]^{2+}$ to form the b series fragments. We have previously noted that an endothermic proton-transfer process can convert $[M + 2H]^{2+}$ into $[M + H]^+$;[18] presumably HeH^+ is the corresponding product ion.[37] Other processes (e.g., dissociation of larger aggregates that are not efficiently injected into the drift tube at lower injection energies) may also contribute to $[M + H]^+$ formation at higher injection energies.

Influence of Injection Voltage on $[M + H]^+$ and $[M + 2H]^{2+}$ Families. Figure 6 shows nested distributions recorded for a mixture of tryptic fragments of myoglobin at injection voltages of 50 and 150 V. Peaks are assigned to peptides that are expected from digestion of the protein (as indicated) by comparing experimental masses (from combined m/z and mobility data) with calculated fragment masses. Over the range of injection voltages used, all expected tryptic fragments (having two or more residues) were observed. It is instructive to compare the major peaks that are observed at different injection voltages. At 50 V there are six major peaks in the $[M + H]^+$ family and seven major peaks in the $[M + 2H]^{2+}$ family that can be assigned to expected fragments. Two-dimensional integration of three 50-V data sets shows that peaks in the $[M + H]^+$ and $[M + 2H]^{2+}$families constitute 23 ± 4 and 77 ± 4% of the ion signal, respectively. At an injection voltage of 90 V (not shown), the distribution of observed peaks shifts to higher m/z ratios and the populations of ions in the $[M + H]^+$ and $[M + 2H]^{2+}$ families are measured to be 43 ± 2 and 57 ± 2%, respectively. At 150 V the percentage of ions in each of these families is 72 ± 2 and 28 ± 2%, respectively. The shift in abundance of these families is consistent with conversion of $[M + 2H]^{2+}$ ions into $[M + H]^+$ ions (as described for bradykinin). The high-injection-voltage $[M + H]^+$ family also shows a series of small peaks (having flight times of ~2.2−3.5 μs) that probably correspond to fragmentation of $[M + 2H]^{2+}$ ions (as observed for bradykinin). For many peptides it is possible to monitor the decrease in the +2 state and corresponding increase in the +1 state. For example, at 50 V, peaks due to $[ALELFR + 2H]^{2+}$ and $[LFTGHPETLEK + 2H]^{2+}$ are large, while $[M + H]^+$ peaks for these peptides are small. At 150 V, the reverse trend is observed: $[M + H]^+$ peaks are large while $[M + 2H]^{2+}$ are small. A survey of digests of eight different proteins shows that distributions do not change substantially for injection voltages of 70 V or below. This suggests that these low-injection-voltage data reflect the distribution of stable ions that are accumulated in the ion trap.

Influence of Trapping Time on Nested Distributions. In a limited series of studies we have examined the influence of trapping time on nested distributions. Studies of bradykinin ions, using low-energy injection conditions, show no significant changes

in the populations of $[M_n + nH]^{n+}$ ($n = 1-3$) multimers over trapping times ranging from 40 to 800 μs. This indicates that multiply charged aggregates are stable at 300 K over long time scales and that collisional excitation in the trap is negligible. Although we observe no large changes in bradykinin multimer populations, some ions appear to be influenced during trapping. Comparison of some peptide digest distributions recorded with and without the trap (at identical injection voltages) shows some differences in ion distributions. In particular, when ions are accumulated for 150 μs it becomes difficult to discern some small (four to six residue) $[M + 2H]^{2+}$ ions that are observed when no trap is used. As mentioned above, the ability of the amino terminus of $[M + H]^+$ to stabilize a second proton in close proximity of a protonated basic residue will decrease with decreasing size. It appears that some small $[M + 2H]^{2+}$ ions are susceptible to loss of a proton (presumably at the less basic N-terminal site) during accumulation in the trap.

Intrinsic Properties of Ions That Limit Separation of Charge-State Families. Separation of ions into charge-state families is intrinsically limited by variations in cross sections that occur with charge state. In the case of peptide digests, where most peptides are observed as singly or doubly protonated ions, a large difference in drift force makes it possible to separate most ions into charge-state families even when the conformation of peptides varies with charge state. For higher charge-state systems this may not be the case. The relative change in drift force between two adjacent charge states decreases with increasing charge. In addition, if conformations expand with increasing charge state in order to minimize Coulombic repulsion energy,[21,38] then mobilities will be dominated by changes in structure rather than charge. Under these conditions, charge-state families will not be observed. An example involving the separation of highly charged protein ions is shown in Figure 7 for a mixture of electrosprayed ubiquitin and myoglobin. Peaks corresponding to the +11 to +22 charge states of apomyoglobin (mol wt = 16 951) and the +6 to +13 charge states of ubiquitin are observed. The results show that there is some reduction in the congestion of peaks; however, the drift times for $[M + nH]^{n+}$ ($n = 7-11$) ions of ubiquitin are similar to those for myoglobin $[M + 2nH]^{2n+}$ ions. Here, the factor of 2 difference in charge state leads to only a marginal separation of these ions. The mobilities of these ions are similar because the cross section-to-charge ratios of the ions are similar. In these types of systems, the mobility-based separation provides an advantage in reducing peak congestion; however, in many cases the advantage is less than is observed for lower charge states.

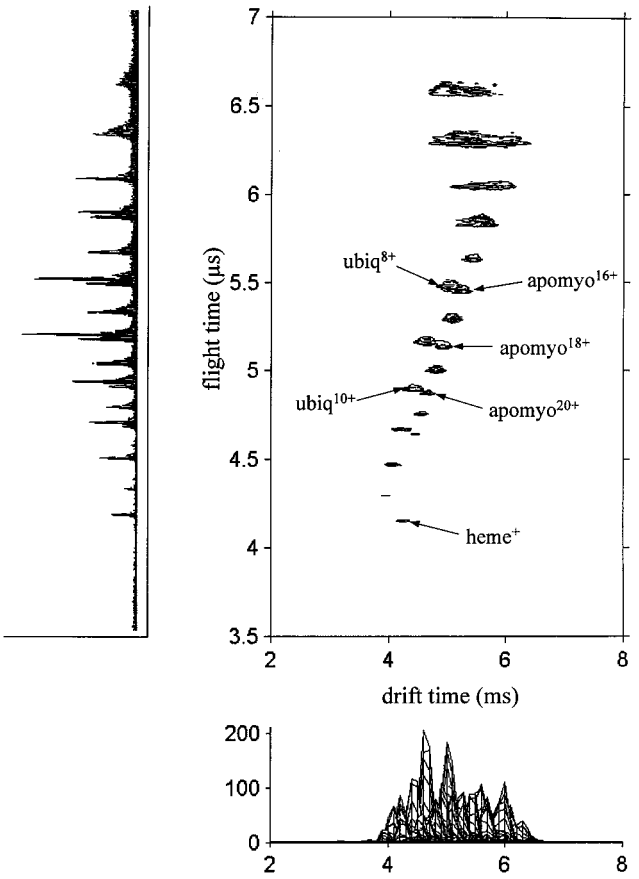

Figure 7. Contour plot of nested data for a prepared equimolar (1×10^{-5} M) mixture of ubiquitin and myoglobin using an injection voltage of 60 V. Other conditions are the same as those in Figure 2.

SUMMARY AND CONCLUSIONS

ESI/ion trap/ion mobility/time-of-flight mass spectrometry techniques have been used to separate and identify components of complex biomolecular mixtures. The methods are shown to be sensitive and rapid. From studies of mixtures having known compositions, we have determined detection limits of 0.5−3.0 pmol for individual components. Most peptides from a mixture of tryptic fragments of cytochrome *c* could be identified in data that were recorded in 60 s. Examples have been given to illustrate advantages of the approach, including the following: (1) reduced peak congestion in mass spectra of electrosprayed mixtures; and (2) assignment of sequences based on comparisons of experimental cross sections to calculated cross sections for trial conformations.

A number of studies have been carried out to deduce how experimental and intrinsic factors influence the ability to separate and detect ions. Studies of individual peptides show that injection voltages of 70−100 V provide sufficient internal excitation to dissociate most noncovalent adducts that are formed during the ESI process. At injection voltages greater than 110 V, a significant fraction of the peptide ions fragment. The influence of injection voltage and trapping time on nested distributions of mixtures of peptides from tryptic digests was also examined. At low injection voltages, peaks in the $[M + 2H]^{2+}$ family dominate the nested distribution; at high injection voltages $[M + H]^+$ ions are favored. An endothermic proton-transfer reaction that forms HeH^+ was invoked to explain these results.

The ability to assign sequences based on mobility data for components of mixtures that cannot be assigned based on *m*/*z*

(38) Covey, T. R.; Douglas, D. J. *J. Am. Soc. Mass Spectrom.* **1993**, *4*, 616.
(39) Jarrold, M. F. *J. Phys. Chem.* **1995**, *99*, 11.
(40) Lee, S., Wyttenbach, T., von Helden, G., Bowers, M. T. *J. Am. Chem. Soc.* **1995**, *117*, 10159.
(41) Tuckerman, M.; Berne, B. J.; Martyna, G. J. *J. Chem. Phys.* **1992**, *97*, 1990.
(42) Cornell, W. D.; Cieplak, P.; Bayly, C. I.; Gould, I. R.; Merz, K. M., Jr.; Ferguson, D. M.; Spellmeyer, D. C.; Fox, T.; Caldwell, J. W.; Kollman, P. A. *J. Am. Chem. Soc.* **1995**, *117*, 5179.
(43) Procacci, P.; Marchi, M. *J. Chem. Phys.* **1996**, *104*, 3003.
(44) Several small peptides having identical compositions but different sequences have recently been resolved on the basis of differences in ion mobilities. See, for example: Asbury, G. R.; Wu, C.; Siems, W. F.; Hill, H. H. Pittcon, New Orleans, LA, March 1−5, 1998, Abstr. 568.

ratios alone is a unique advantage of the gas-phase separation approach. The basic approach is analogous to the method used to deduce structures for different isomers for a number of atomic clusters and complex ion systems.[39,40] For peptide assignment, this approach is currently constrained by the reliability of molecular modeling force fields, algorithms for finding energetically favorable conformations, and accuracy of the method used to calculate cross sections for trial conformers, requiring that computationally expensive calculations be undertaken for definitive assignments. Tremendous progress in these areas has been made in recent years.[41−43] With additional improvements it seems likely that many different peptide sequences that have indistinguishable molecular weights can be identified with this integrated approach. The ability to resolve different sequences of oligomers having identical molecular weights[44] by differences in their mobilities and assign peaks based on comparisons with molecular modeling would have applications in a wide range of separations problems including analysis of small combinatorial libraries.

ACKNOWLEDGMENT

This work is supported by a grant from the National Institute of Health (Grant 1R01GM55647-01) with additional support from the Petroleum Research Fund administered by the ACS (Grant ACS-PRF 31859-G4).

Received for review August 13, 1998. Accepted November 11, 1998.

AC9809175